Resource-Efficient Coverage Path Planning for UAV-Based Aerial IoT Gateway

Nurul Saliha A. Ibrahim* and Faiz A. Saparudin

Universiti Tun Hussein Onn Malaysia, Johor, Malaysia; Email: faizs@uthm.edu.my (F.A.S.)
*Correspondence: salihaamani96@gmail.com (N.S.A.I.)

Abstract—Unmanned Aerial Vehicles (UAVs) have a lot of potential for developing new applications in a variety of fields, such as traffic monitoring, security, and military applications. In the vast nature of the Internet of Things (IoT) network, UAVs could work as Aerial Gateway (AG) for communications among low-powered and distributed ground IoT Devices (IDs). This research concentrates on the path planning and deployment system that may facilitate decision-making and guaranteed resource-efficient UAV mission assignment in serving ground IDs. Due to limited resources, it is essential to take into account several factors when designing such a system, including the AG flight time, the coverage radius, and the ground-to-air system's achievable data rate. As a result, the Energy Efficient Coverage Path Planning (EECPP) algorithm has been proposed. The EECPP is composed of two algorithms: the Stop Point Prediction Algorithm using K-Means, and Path Planning Algorithm using Particle Swarm Optimization. The outcome demonstrates that, in terms of total flight distance, EECPP outperforms Close Enough Traveling Salesman Problem (CETSP) by 19.99%. EECPP reduced energy usage by an average of 56.15% as opposed to Energy-Efficient Path Planning (E2PP). Due to its mobility nature with the addition of effective path planning, the AG is able to hover at each stop point, making it ideal for usage in crowded regions with high demand, emergency circumstances, and distant locations with no access to fixed base stations.

Keywords—path planning, resource-efficient, unmanned air vehicles

I. Introduction

In recent years, unmanned aerial vehicles (UAVs) have gained popularity in a variety of public applications, including aerial surveillance, traffic control, photography, package delivery, and communication platforms [1]. UAVs in wireless communications especially in the internet of things (IoT) network has attracted a lot of attention from both corporations and academia recently. IoT is a massive collection of smart embedded devices that are connected to the Internet and provide unique services to satisfy the consumer's needs, with one trillion gadgets estimated to be in use worldwide by 2025 [2]. There are four representative scenarios in UAV-assisted communication system, including UAVs as aerial gateways (AG), UAVs as mobile relays, UAVs as motorial energy sources, and UAVs as aerial caches [3].

The use of UAVs as AGs in substitution for existing terrestrial base stations can improve network coverage, particularly in IoT communication systems. Due to the fixed location of the terrestrial base stations and its weak line-of-sight (LoS), signal blockage and shadowing have become a challenge. By considering the height, AG can successfully establish LoS communication linkages with terrestrial users [4]. AG may alter the area of coverage as needed while maintaining LoS, owing to its mobility characteristic, which makes it easy to change its altitude [5]. Due to their adaptable altitude, AG may be quickly deployed to serve IoT devices without being hindered by geographic constraints, hence minimizing signal blockage and shadowing [6]. The use of UAVs in serving wireless communication is currently able to provide many opportunities to mitigate communication issues with a cost-effective approach. A study conducted in [7], showed a reduction of 56% in the total transmit power of IoT devices for reliable uplink communications compared to fixed base station.

Additionally, in some areas, building out an entire cellular infrastructure can be exceedingly expensive. Therefore, AG deployment becomes advantageous in solving this problem as it eliminates the requirement for costly towers and infrastructure [8]. Unexpected demand in certain coverage areas can lead to insufficient network resources which then deteriorates the service quality in that particular area. With the implementation of AG in the system, the service demand not only depends on the ground base station but also can be distributed to the aerial base station, hence improving the quality of service. AG can be deployed to complement existing cellular systems by providing additional capacity to hotspot locations as well as to provide network coverage in emergency and public safety situations [8].

In IoT communication system, specific requirements such as long range, low data rate, low power consumption, and cost effectiveness exist. In low power wide area networks (LPWAN), the maximum data rate for Sigfox, LoRaWAN, and NB-IoT is 100 bps, 50 kbps, and 200 kbps respectively [9]. However, due to their low transmit power

Manuscript received December 7, 2022; revised February 21, 2023, accepted March 30, 2023.

and short battery life, IoT devices (IDs) are unable to transmit data remotely to ground base stations. By programming AG to move toward IoT devices, it creates a create reliable connections with low transmit power from IoT devices [7]. If the distance between the take-off points and the target point is not taken into account, it may result in loss of energy as traveling to the points will be time-consuming [10]. The flight duration of the AG can be reduced with an appropriate resource-efficient path planning method, allowing the AG and IoT device to perform at their maximum potential.

In general, AG contributes in improving network coverage and reducing operating cost and overall process time. Unfortunately, due to an ineffective resource management system, wastage of energy, power, and time consumption still occur in path planning and data transmission process involving AG. To deal with this problem, this research was conducted in order to improve the decision-making, including UAV path planning and IoT data collection. For energy efficiency improvement, the flight time of AG needs to be minimized [11, 12] with sophisticated path planning and management system. The system is expected able to help users utilize resources more efficiently in ensuring competitiveness and quality of service of IoT communication system. The contributions of the research are listed below:

- This research proposes an automated cluster determination algorithm that ensures maximum radius based on achievable data rates, ensuring optimal communication between ground IoD and AG.
- By utilizing the algorithm-generated shortest path, this research achieves a significant reduction in travel time and total distance, resulting in a significant reduction in energy consumption.
- The implementation of EECPP in this research successfully reduces the total energy consumption required for data transmission from IDs to AG. As a result, this research offers an efficient and feasible solution for obtaining remote data.

II. Related Work

In UAV path planning, the performance metrics and evaluation method are essential in determining the effectiveness of the algorithm or method. From path planning method presented in [13], Ji *et al*. evaluated the performance of the algorithm based on energy consumption, which influenced by the distance and the angle of heading change of the UAV. The algorithm, called the Energy Consumption Estimation Model Based on Distance and The Angle of Heading Change (ECEMBDA), is based on Greedy or Djikstra algorithm. The results showed that the ECEMBDA planned path is more energy efficient and smoother than the conventional method, saving roughly 12.21 percent of the UAV's energy usage.

Zhan *et al*. [14] assessed the performance of energy consumption and completion time, where both of two are affected by the task data size as they are directly proportional to it. The objective was to minimize the total energy consumption of the UAV via jointly optimizing the design variables, including the UAV trajectory, velocity, acceleration, resource allocation, offloading scheduling, and completion time. The results demonstrated significant performance improvements over the baseline schemes, as well as revealing the trade-off between UAV completion time and energy usage for the mobile edge computing system. The joint optimization of design variables has the potential to achieve significant energy savings, reducing operational costs and improving the overall performance of the wireless system.

Shivagan *et al*. conducted a study [15] on task scheduling involving multiples UAVs and evaluates the number of UAVs deployed and the whole system's energy consumption by introducing the algorithm to schedule their deployment. To optimize the flight path and minimize UAVs energy consumption, the research considers reducing the number of turns made by the UAV using Genetic Algorithm. The results revealed that the proposed algorithm uses 2 to 5 times less energy than the greedy algorithm.

Study by Pouded *et al*. [16], aimed to reduce the energy consumption of sensors and minimize the network latency. They present a hybrid path planning technique for efficient data collection in emergency scenarios by ensuring the shortest collision-free path for UAVs. The probabilistic roadmap (PRM) algorithm is utilized to create the shortest trajectory map. The improved artificial bee colony (ABC) algorithm is used to enhance different path constraints in a three-dimensional environment. Simulation findings showed that the proposed technique outperformed the PRM and standard ABC schemes significantly in terms of flight time, energy consumption, convergence time, and flight path. This research highlights the importance of considering path planning techniques in UAV mission planning for efficient data collection, particularly in emergency scenarios. The use of hybrid techniques that combine different algorithms can help to optimize UAV trajectories, minimize energy consumption, and improve the overall performance of the system.

III. System Specification and Consideration

Among several types of UAVs, quadrotor UAV has been chosen as it has simple construction, good motor performance, vertical take-off, and land ability, and it is also easy to build and maintain [10]. To deploy the AG to cover all IoT devices in an effective and resource-efficient manner, K-means clustering was used. Once the centroid of each cluster was identified, path planning algorithm was needed to link each cluster for AG deployment. The path planning problem was based on Traveling Salesman Problem (TSP). It is computationally complex to select the optimal path from a large number of nodes, but easier to solve after converting it to TSP [17]. The TSP was then solved using the Particle Swarm Optimization (PSO) algorithm.

A. System Model

The system model as illustrated in Fig. 1 can be divided into two layers, namely ground level and air level. The height between the ground and air level was set at 100 m in free space where there are no obstacles. By

considering an IoT device consisting of ID_n as n = (0, 1, 2, …, N) deployed within a geographical area. The total number of IDs in the map is represented by ID_N. The location of IDs and AG are given by X_{IDn}, X_{IDn}) and (X_{AG}, Y_{AG}, h_{AG}), respectively. The location of IoT devices was assumed known by the AG. The IDs were grouped into clusters, Ck as k = (0, 1, 2, …, K) and k is the number of clusters. At ground level, the centroid location was determined for each cluster, and perpendicular to it with a height of 100 m, which is the stop point, Uk as k = (0, 1, 2,…, K) where AG needs to be visited. The problem formulation is to minimize the energy consumption of ID and AG while ensuring all data from IDs are collected. To obtain minimum energy consumption, the optimal propulsion power of AG is determined, and the travel time of the AG is minimized by reducing the travel distance. The process of obtaining the path with efficient energy usage is being done offline, thus the cost of finding the optimal path will not deplete the UAV's battery.

B. Objective Function

The objective function is to minimize the energy consumption of IDs and AG using the Eq (1) by reducing the distance and time travel of the AG.

$$\min E_{consumed} = \sum E_{ID} + E_{AG}$$

Such that

$$\sum E_{ID} = N_{ID} \times P_{ID} \quad (2)$$

$$E_{AG} = P_{AGmin} T_{total} \quad (3)$$

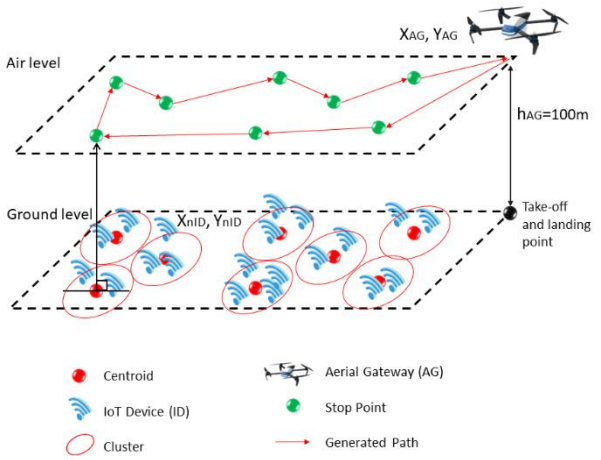

Figure 1. Aerial gateway to serve ground IoT devices network topology

where, N_{ID} is the number of IDs in the system and P_{ID} = 8mJ denotes the energy consumed by each ID to transmit 100 bytes of data below a radius of 500 [18]. P_{AGmin} = 105.801 Watts the propulsion power of the AG, which is required to maintain the AG in the air and allow it to move around [19].

C. Problem Formulation

T_{total} is the total time consumed to finish covering all of the IDs, T_{total} can be calculated using Eq (4).

$$T_{total} = T_{wait} + T_{travel} \quad (4)$$

where T_{wait} is total waiting time for all cluster and T_{travel} is total time needed to travel from stop point 0 to J. T_{travel} can be acquired using Eq (5)

$$T_{travel} = V_{AG} D_{travel} \quad (5)$$

D_{travel} is the distance traveled between multiple stop points. Step in obtaining D_{travel} is explained in Eq. (19). V_{AG} =8m/s is the optimal speed of the AG which determined in Eq (13). Total waiting time for all cluster can be modelled using Eq (6)

$$T_{wait} = \sum_{i=0}^{J} t_{0wait} + t_{1wait} + \cdots + t_{Jwait} \quad (6)$$

where t_{jwait} is the total waiting time for each cluster and it can be determined using Eq (7)

$$t_{jwait} = \sum_{i=0}^{n} t_{ID0wait} + t_{ID1wait} + \cdots + t_{IDnwait} \quad (7)$$

Eq. (7), the $t_{IDnwait}$ is the waiting time of AG in order to obtain data from each ID where it can be obtained using Eq. (8)

$$\text{Waiting Time for each ID } (t_{IDnwait}) = \frac{\text{packetsize}}{R_{IDn}} \quad (8)$$

Such that the packet size = 100 bytes. Furthermore, R_{IDn} denotes the achievable data rate for data transmission from each ID to AG based on [14] and is shown in Eq (9).

$$R_{IDn} = BW log_2 \left[1 + \frac{\gamma}{[h^2 + (X_{IDn} - X_{AG})^2 + (Y_{IDn} - Y_{AG})^2]^{\frac{\alpha}{2}}} \right] \quad (9)$$

where bandwidth, BW=125 kHz, γ is the SNR value per unit meter = 66.71 dB and α=2 is path loss exponent in free space. BW value of 125kHz is chosen as low bandwidth offers long range transmission and higher sensitivity as compared to higher bandwidth [20, 21]. The data rate obtained, R_n, is expected to be at minimum value of 300bps. Signal-to-Noise Ratio (SNR) can be obtained using

$$\text{Signal to Noise Ratio (SNR)} = P_r + G_C - AWGN \quad (10)$$

The $SNR\ limit$ of the system is set to 20 dBm as LoRa can modulate signal until 20 dBm below noise floor [22]. $AWGN$ = -128 dBm denotes the Additive white Gaussian Noise of the system, and P_r is the power received by the AG. P_r can be calculated by

$$Power\ Received\ (P_r) = Pt - L_{bf} \quad (11)$$

While channel gain, Gc can be acquired using

$$\text{Channel Gain } (G_C) = 10 log_{10} \left(\frac{\lambda}{4\pi^2} \right)^2 - 20 log_{10}(d) \quad (12)$$

where d is the distance between each ID to AG, while 0.3276 is the wavelength of the channel frequency. L_{bf} in P_r formula in Eq. (11) stands for Free Space Path Loss. The parameter's assumption values used above are tabulated in Table I.

TABLE I. LIST OF PARAMETERS VALUE

Parameter	Value
Frequency, f	919 MHz
Wavelength, λ	0.3276
Bandwidth, BW	125 kHz
Data Rate, Rid	300 bps to 50 kbps
Packet Size,	100 bytes
SNR Limit	-20 dBm
Transmit Power, Pt	14 dBm
SNR Value Per Unit Meter, γ	66.71 dB
Path Loss Exponent in Free Space, α	2
Maximum Cluster Radius, R	283 meters
AG Height	100 meters
Optimal Speed of AG, V_{AG}	8 m/s
Minimum AG power consumption, P_{AGmin}	105.801 Watt
Tip speed of the rotor blade, U_{tip}	120m/s
Fuselage drag ratio, d_0	0.6
Rotor solidity, s	0.05
Air density, ρ	1.225 kg/m^3
Rotor disc area, A	0.503m^2
Profile drag coefficient, δ	0.012
Blade angular velocity	300 rad/s
Rotor Radius, r	0.4m
Incremental correction factor to induce power, k	0.1
Weight of the UAV, W	13.53 Newton

D. AG Power Consumption Model

In general, there are two major components that influences the UAV energy consumption. The first is energy used in communication, which includes circuitry, signal processing, and signal receiving and transmission. The other is propulsion energy, which is required to maintain the UAV in the air and allow it to move around. The energy used in communication can be neglected as typically much lower than the propulsion energy in practice [19]. P_{AGmin} is formulated in Eq. (13) using formula from [19, 23, 24]:

$$P_{AGmin} = P_0\left(1+\frac{3{V_{AG}}^2}{U_{tip}^2}\right)+P_i\left(\sqrt{1+\frac{{V_{AG}}^4}{4v_0^4}}-\frac{{V_{AG}}^2}{2v_0^2}\right)^{\frac{1}{2}}+\frac{1}{2}d_0\rho sA{V_{AG}}^3 \quad (13)$$

where P_0 and P_i are two constants used in calculating the blade profile power and induced power in hovering status, and can be calculated using Eq. (14) and Eq. (15) respectively. U_{tip} denotes the tip speed of the rotor blade, v_0 is known as the mean rotor induced velocity in hover as in eq (16), d_0 is the fuselage drag ratio, and s is the rotor solidity which is the ratio of the total blade area to the disc area. ρ is the air density, and A denote rotor disc area.

$$P_0 = \frac{\delta}{8}\rho sA\Omega^3 r^3 \quad (14)$$

where δ is the profile drag coefficient, Ω denotes the blade angular velocity, and r is the rotor radius.

$$P_1 = (1+k)\frac{W^{\frac{3}{2}}}{\sqrt{2\rho A}} \quad (15)$$

where k is the incremental correction factor to induced power, $k = 0.1$.

$$v_0 = \sqrt{\frac{W}{2\rho A}} \quad (16)$$

where W is the weight of the AG and payload. The optimal speed of the AG, V_{AG} is determined by substituting the equation in (13) with the range of minimum to maximum speed of AG, which is from 0m/s to 20m/s. From the graph obtained in Fig. 2 below, the optimal speed, V_{AG} that able to minimizes the power consumption of AG is approximately 8m/s.

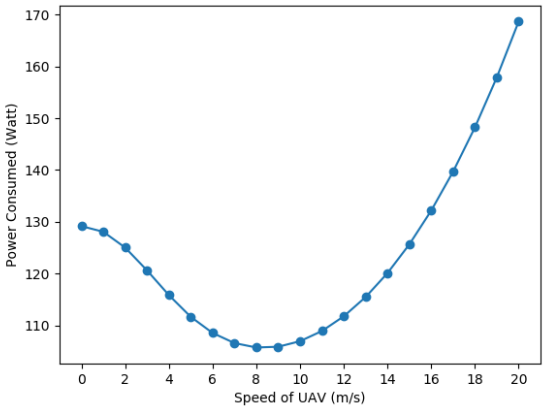

Figure 2 Power consumed against speed of UAV.

IV. ENERGY EFFICIENT COVERAGE PATH PLANNING ALGORITHM

The Energy Efficient Coverage Path Planning Algorithm (EECPP) is divided into two sections, namely Stop Point Prediction Algorithm using K-Means and Path Planning Algorithm using PSO.

A. Stop Point Prediction Uisng K-Means Algorithm

Algorithm 1 Stop Point Prediction Using-K-Means

```
Input:
N_ID = {ID_1, ID_2…ID_N} //set of IDs to be clustered
K_1 //minimum predicted number of clusters
K_2 //maximum predicted number of clusters
R //maximum cluster radius
Output:
K //actual number of clusters
C = {C_1, C_2, ….C_K} //set of clusters
J = {J_1, J_2, …J_K} //set of stop point / centroid
For K in range of K_1 to K_2 do
        Assign initial set of clusters
        For each cluster do
            Determine cluster centroid
            Calculate distance from each ID to centro
            Group based on minimum distance
            If no IDs move group then
                If minimum distance from ID to
                centroid > maximum cluster radius
                then
                    K=K+1
                    Go to (10)
                End If
                Else Go to(13)
            End If
        End For
End For
```

The Stop Point Prediction using-K-Means is explained in Algorithm 1. The first stage is to initialize the number

of IDs to be clustered (NID), the range of predicted number of clusters (K1 to K2), and the maximum cluster radius (R). In order too obtain the actual number of cluster (K), the iteration will be done until the IDs on the map are included in the cluster without exceeding the maximum radius from the centroid.

For each K value in range of K1 to K2, a random set of clusters (C) is initialized and the centroid coordinates (J) are then determined. In the next step, the actual distance between the AG location or the centroid to all IDs are calculated using Euclidean distance metric function. In order to ensure that the SNR value of the communication is always in achievable range of -20 dB to 10 dB [22], the maximum distance from each ID to AG need to be at 300 meters. The height of the AG is set to 100 meters as it is the most common height used by researchers [23-25], and it complies with the Civil Aviation Authority Malaysia that small unmanned aircrafts should not fly over 122 meters [26]. The maximum radius of each cluster needs to be at 283 meters or less, so that every time the AG visited any cluster, it can cover all the IDs in that cluster without exceeding the maximum radius and minimum SNR.

The height of the AG (h) is fixed at 100 m from the ground and n refers to the ID number. Next, the IDs are then arranged based on the shortest distance. Lastly, the distance between the AG location or the centroid to all IDs are compared to the maximum cluster radius. If the distances from current K number exceed the maximum radius, the iteration will proceed to the next K number until the radius is satisfied. The centroid of the clusters consisting of J numbers is referred to as the stop points for the AG.

B. Path Planning Algorithm Using Particle Swarm Optimization (PSO)

The AG is assumed to visit a set of J stop points, which are clustered by K-means and connected by the shortest path while managing the resource in an efficient manner. In this situation, the resource-efficient path planning can be obtained by solving the TSP using PSO algorithm.

Algorithm 2 presents the details of PSO algorithm, which begins by initializing the number of particles, their velocity and maximum epoch value. The epoch value, which determines the duration of the algorithm will be run, is set to 10000. The current fitness value for each particle is then evaluated in iterations based on the cost to be optimized to solve the TSP problem. The velocity reflects the distance, position, and speed of the particle at each iteration [27] and can be expressed using Eq. (17).

$$V_{m+1}^{i} = wV_m^i + c_1 r_{1_m}(pbest_m^i - X_m^i) + c_2 r_{2_m}(gbest_m^i - X_m^i) \quad (17)$$

where, V_m^i and X_m^i represent velocity and position of i^{th} particle in m^{th} iteration, respectively; personal best, or $pbest_m^i$ denotes the previous best position found by the particle itself (particle memory); global best, $gbest_m^i$ represents the previous best solution found by the entire population (swarm memory); W = 0.4 represents the inertial weight of the particles at the previously attained position; c_1=1.5 and c_2=2 represent acceleration constants; and r_{1m} and r_{2m} represent random numbers in the range of [0,1] [28].

The new position of each particle, X_{m+1}^i is then updated based on the latest velocity value to obtain the latest gBest, until it reaches its stopping criteria using Eq. (18):

$$X_{m+1}^i = X_m^i + V_{m+1}^i \quad (18)$$

The stopping criteria in this research in maximum number of epochs. The gBest obtained is the summary of distance traveled between multiple stop points and it can be expressed by

$$D_{travel} = \sum_{i=0}^{j} d_0 + d_1 + \cdots + d_j \quad (19)$$

After achieving the D_{travel} value, it is integrated into Eq. (5) to obtain the total time travel.

Algorithm 2 Path Planning Algorithm Using Particle Swarm Optimization

```
Input:
K //actual number of clusters
J = {J1, J2, …Jk} //set of stop point / centroid
P //particle count
V_Max //maximum velocity change allowed
Max_epoch //maximum number of iterations
Output:
Shortest path
For each particle (P) do
    Initialize position and velocity randomly
End For
For each particle (P) do
    Evaluate the fitness function //the total distance connect all stop point
    If current fitness value better than pBest then
        Assign current fitness as new pBest
    Else keep previous pBest
    End If
End For
For each pBest do
    If current pBest better than gBest then
        Assign pBest value to gBest
    Else keep gBest
    End If
End For
For each particle (P) do
    Update Particle velocity
End For
Until stopping criteria satisfied
```

Generation Algorithm is the make_blob function which is based on Gaussian distribution. In this function, there are several parameters that can be adjusted to obtain the desired output. The user can set the number of ID samples, take-off and landing location of the AG. The number of ID generated was later denoted by $N_{ID} = (ID_1, ID_2, \ldots ID_N)$. The dispersion of the ID, denoted by β, can also be adjusted and is influenced by the number of centers initially expected by the user, $E_{centers}$ and the number of IDs, N_{ID}, using equation in Eq. (20):

$$\text{cluster dispersion}, \beta = \left(\frac{E_{centers}}{N_{ID}}\right) \times 100 \quad (20)$$

The function of the dispersion percent is to determine whether the map would be dense or sparse, mimicking real-life scenarios such as rivers, lakes, cities, and forests as desired by the user.

V. Result

A. Node Generation and Algorithm Implementation

By implementing the Location Generation Algorithm of the IDs, various maps with different situations were obtained. Take-off and landing points were set at coordinate [10,10] with 100 IDs. The simulation maps were set to 1000 m^2 with the dispersion percentage, β of 25, 50, 75, and 100, as shown in Fig. 3 (a) - (d) respectively.

B. Energy Efficient Coverage Path Planning Anaysis

From the ID locations obtained on each map V(A), the IDs were then clustered based on the Stop Point Prediction Algorithm using K-Means. This algorithm covered processes on the ground level. The range of cluster was initially set between 2 to 100 clusters. And using the prediction of elbow method [29], the actual value of the optimum cluster was determined, resulting in nine clusters. The maximum distance of each ID was set to be 300 m from the AG stop points. The results in Table II indicate the number of optimum clusters with their centroid location.

By tuning the particle value and maximum epoch 10000 in the path planning algorithm, for the map of 25% dispersion percentage, the shortest path obtained were 8, 3, 7, 6, 4, 1, 5, 2 with a total distance of 2962.867 m. The total distance represents the distance for the AG to travel from the take-off point to all stop points and return to its initial point. The map for shortest path is illustrated in Fig. 4.

TABLE II. Centroid's Location for Map WTH Dispersion Percentage of 25%

Cluster Number	Cluster Color	X Coordinate	Y Coordinate
8		10.0	10.0
3		138.702	640.718
7		215.329	878.509
6		364.742	664.144
4		755.840	739.979
0		619.692	493.929
1		774.991	263.414
5		519.858	279.853
2		256.412	222.098

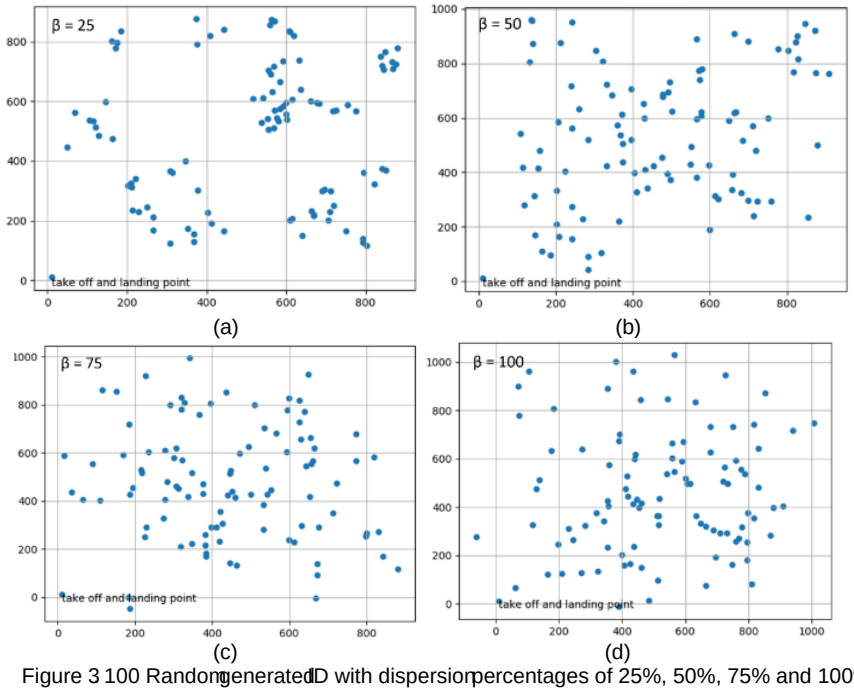

Figure 3 100 Random generated ID with dispersion percentages of 25%, 50%, 75% and 100%

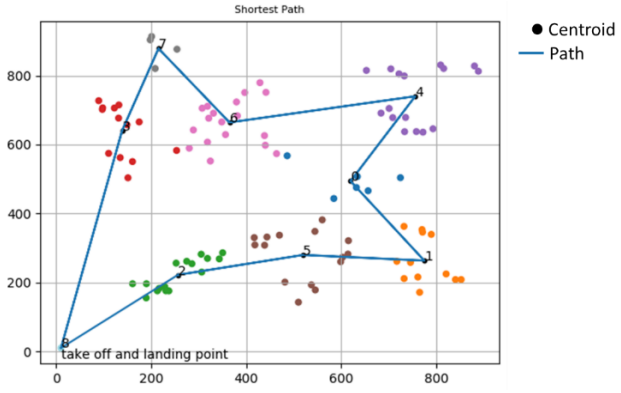

Figure 4 Map for shortest path.

The total distance traveled, time taken, energy consumed, and energy efficiency of AG to cover 100 IDs on the map with dispersion percent, β of 25, 50, 75 and 100 are being analyzed and the values are tabulated in Table III. It can be deduced that the distance traveled by the AG increases as the dispersion percent increase.

TABLE III. Total Distance Traveled, Time Taken, Energy Consumed, and Energy Efficiency

B (%)	D_{travel} (Meter)	T_{total} (Second)	$E_{consumed}$ (Joule)	Energy Efficiency (bit/Joule)
25	2962.867	465.582	57363.390	1.395
50	3230.34	586.966	62101.629	1.288
75	4188.616	689.37	72936.035	1.097
100	5131.008	812.814	85996.521	0.93

C. Analysis on Distance Traveled

The efficiency of the EECPP was analyzed by comparing its results with other methods. In this study, the total distance obtained was compared with Close Enough Traveling Salesman Problem (CETSP) method [30] which implements branch-and-bound algorithm to cover the desired stop points. The CETSP method involves generating multiple map scenarios using different percentage of dispersion and dividing the points into grids or quadrants, with the UAV only visiting the center of the grid containing the points. For the IDs generation, 20 IDs were used with a β ranging from 10% to 100% in increments of 10%. Table IV shows the distances obtained using the EECPP method compared to those obtained from the CETSP method

TABLE IV. DISTANCE TRAVELED USING EECPP COMPARED TO CETSP

'LVSHUVLRQ SH	CETSP (meter)	EECPP (meter)
10	1472.3	1462.39
20	2281.9	1927.72
30	2858.6	1996.63
40	2765.5	2070.91
50	2881.7	2311.18
60	3073.9	2467.28
70	3229.3	2532.53
80	3253.8	2498.03
90	3163.8	2693.58
100	3378.7	3111.08

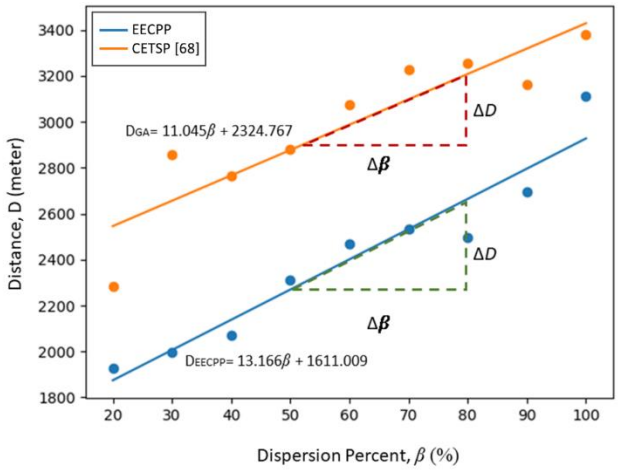

Figure 5 Linear fitting graph for predicting the distance value of based on the changes in dispersion percentage (β).

TABLE V. GOODNESS OF FITTING FOR CETSP AND EECPP

	CETSP	EECPP
Multiple R	0.903866	0.961346
R Square	0.816974	0.924186
Adjusted R Square	0.790827	0.913355
Standard Error	153.0542	110.405298

Linear fitting techniques were applied to the result to predict the distance values based on the dispersion percentage (β). The efficiency of the algorithm was determined by examining the change of D relative to β; a smaller change of D relative to β indicates higher efficiency of the algorithm. The linear fitting graph for dispersion percentage against the distances for CETSP and EECPP is illustrated in Fig. 5 and its goodness of fitting is presented in Table V.

The analysis of the linear fitting graph revealed that EECPP reduced the average distance by 9.9% compared to CETSP. In a regression model, R-Squared is a statistical measure of fit that shows how much variance in a dependent variable is represented by the independent variables. In this context, it shows how much the distance traveled by CETSP and EECPP is represented by the dispersion percentage. From the value in Table V, The R square of EECPP is higher than the R square of CETSP, thus, it indicates that the distance traveled by EECPP is better represented by the dispersion percentage.

D. Analysis on Energy Consumption

TABLE VI. ENERGY CONSUMED BY EECPP COMPARED TO E2PP

Number of Nodes	E2PP (Joule)	EECPP (Joule)
30	46800	18812.01
40	50400	20895.62
50	54000	26972.91
60	63000	27834.01
70	73800	32320.2

To assess the efficiency of EECPP in minimizing the energy consumption, the results were compared with the Energy-Efficient Path Planning (E2PP) method [13]. E2PP estimates the energy consumption of a UAV to fly from one node to another without grouping the nodes, which requires more energy to finish the entire process. E2PP method results in huge energy consumption as compared to EECPP. Table VI presents the energy consumed by the EECPP algorithm compared to E2PP algorithm.

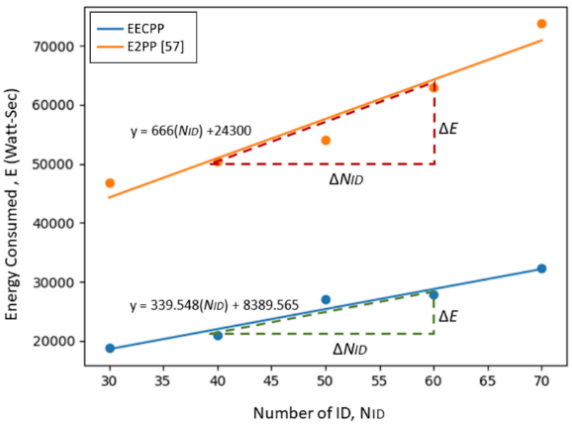

Figure 6 Linear fitting graph for predicting the energy consumption based on the changes in number of ID (N_{ID}).

TABLE VII. GOODNESS OF FITTING FOR E2PP AND EECPP

	E2PP	EECPP
Multiple R	0.968334	0.980299
R Square	0.937671	0.960987
Adjusted R Square	0.916895	0.947982
Standard Error	3134.964116	1249.075

Fig. 6 illustrates the linear fitting graph for energy consumed against the number on nodes while its goodness of fitting is presented in Table VII.

Fig. 6 indicates that the change in energy consumed over the number of IoD of EECPP was smaller, implying that EECPP method promoted more efficient energy consumption at greater number of IoD than E2PP algorithm. The average percentage of energy reduced by EECPP was 56.15%, according to the analysis of the linear fitting graph. From the values in Table VII, The R square of EECPP is higher than the R square of E2PP, thus, indicates that energy consumed by EECPP is represented better by the number of nodes on map.

VI. Discussion and Conclusion

In conclusion, the EECPP method which implemented K-Means clustering and PSO in solving TSP provided resource-efficient path planning for UAVs as aerial gateway to serve ground IoT devices. By clustering the IDs into multiple groups based on achievable communication, it reduced the number of stop points that the AG must visit. EECPP is able to outperform CETSP by 19.99% more efficient in terms of total distance. For energy consumption, at higher number of IDs on the map, EECPP performed better by providing more efficient energy consumption compared to the E2PP algorithm. In addition, the EECPP method reduced up to 56.15% of energy consumption in contrast to the E2PP algorithm. The mobile nature of AG enabled it to hover at each stop points based on the efficiently constructed path, thus making it suitable for implementation in remote areas, where fixed base station is not available, crowded area with high demand, and also in emergency situation. For future work, the algorithm can be improved to include interference management from other wireless devices to ensure its effectiveness in real world scenarios.

Conflict of Interest

The authors declare no conflict of interest.

Author Contributions

Nurul Saliha Amani contributed to the software setup and algorithm development for the optimal solution, as well as the initial paper writing. Faiz Asraf contributed to validating the research outcome, revising, and fine-tuning the manuscript. All research activities were conducted under the supervision of Faiz Asraf Saparudin. All authors have approved the final version of the paper.

Funding

This research was supported by Universiti Tun Hussein Onn Malaysia (UTHM) through Tier 1 (vot Q178) and RE-GG (vot Q200).

References

[1] Y. Zeng, J. Lyu, and R. Zhang, "Cellular-connected UAV: Potential, challenges, and promising technologies," *IEEE Wirel. Commun.*, vol. 26, no. 1, pp. 120–127, 2019, doi: 10.1109/MWC.2018.1800023.

[2] A. Kumar *et al.*, "Revolutionary strategies analysis and proposed system for future infrastructure in internet of things," *Sustain.*, vol. 14, no. 1, 2022, doi: 10.3390/su14010071.

[3] H. Wang, G. Ding, F. Gao, J. Chen, J. Wang, and L. Wang, "Power control in UAV-supported ultra dense networks: communications, caching, and energy transfer," *IEEE Commun. Mag.*, vol. 56, no. 6, pp. 28–34, 2018, doi: 10.1109/MCOM.2018.1700431.

[4] M. Mozaffari, W. Saad, M. Bennis, and M. Debbah, "Wireless communication using Unmanned Aerial Vehicles (UAVs): Optimal transport theory for hover time optimization," *IEEE Trans. Wirel. Commun.*, vol. 16, no. 12, pp. 8052–8066, 2017, doi: 10.1109/TWC.2017.2756644.

[5] M. Mozaffari, W. Saad, M. Bennis, and M. Debbah, "Unmanned aerial vehicle with underlaid device-to-device communications: Performance and tradeoffs," *IEEE Trans. Wirel. Commun.*, vol. 15, no. 6, pp. 3949–3963, 2016, doi: 10.1109/TWC.2016.2531652.

[6] M. Mozaffari, W. Saad, M. Bennis, and M. Debbah, "Mobile Unmanned Aerial Vehicles (UAVs) for energy-efficient internet of things communications," *IEEE Trans. Wirel. Commun.*, vol. 16, no. 11, pp. 7574–7589, 2017, doi: 10.1109/TWC.2017.2751045.

[7] M. Mozaffari, W. Saad, M. Bennis, and M. Debbah, "Mobile Internet of Things: Can UAVs provide an energy-efficient mobile architecture?" in *Proc. 2016 IEEE Glob. Commun. Conf. GLOBECOM 2016*, doi: 10.1109/GLOCOM.2016.7841993.

[8] M. Mozaffari, W. Saad, M. Bennis, Y. H. Nam, and M. Debbah, "A tutorial on UAVs for wireless networks: applications, challenges, and open problems," *IEEE Commun. Surv. Tutorials*, vol. 21, no. 3, pp. 2334–2360, 2019, doi: 10.1109/COMST.2019.2902862.

[9] K. Mekki, E. Bajic, F. Chaxel, and F. Meyer, "A comparative study of LPWAN technologies for large-scale IoT deployment," *ICT Express*, vol. 5, no. 1, pp. 1–7, 2019, doi: 10.1016/j.icte.2017.12.005.

[10] R. L. Galvez, E. P. Dadios, and A. A. Bandala, "Path planning for quadrotor UAV using genetic algorithm," in *Proc. 2014 Int. Conf. Humanoid, Nanotechnology, Inf. Technol. Commun. Control. Environ. Manag. HNICEM*, pp. 1–6, 2014, doi: 10.1109/HNICEM.2014.7016260.

[11] S. Ahmed, A. Mohamed, K. Harras, M. Kholief, and S. Mesbah, *Energy Efficient Path Planning Techniques for UAV-based Systems With Space Discretization*, 2016. doi: 10.1109/WCNC.2016.7565126.

[12] J. Modares, F. Ghanei, N. Mastronarde, and K. Dantu, "UB-ANC Planner: Energy efficient coverage path planning with multiple drones," in *Proc. IEEE Int. Conf. Robot. Autom.*, 2017, pp. 6182–6189, doi: 10.1109/ICRA.2017.7989732.

[13] X. Ji *et al.*, "E2PP: An energy-efficient path planning method of UAV-assisted data collection," *Secur. Commun. Networks*, 2020, doi: 10.1155/2020/8850505.

[14] C. Zhan, H. Hu, X. Sui, Z. Liu, and D. Niyato, "Completion time and energy optimization in the UAV-enabled mobile-edge computing system," *IEEE Internet Things J.*, vol. 7, no. 8, pp. 7808–7822, 2020, doi: 10.1109/JIOT.2020.2993260.

[15] R. Shivgan and Z. Dong, "Energy-efficient drone coverage path planning using genetic algorithm," in *Proc. IEEE Int. Conf. High Perform. Switch. Routing, HPSR*, vol. 2020-May, 2020, doi: 10.1109/HPSR48589.2020.9098989.

[16] S. Poudel and S. Moh, "Hybrid path planning for efficient data collection in UAV-aided WSNS for emergency applications," *Sensors*, vol. 21, no. 8, 2021, doi: 10.3390/s21082839.

[17] Y. Xu and C. Che, "A brief review of the intelligent algorithm for traveling salesman problem in UAV route planning," in *Proc. 2019 IEEE 9th Int. Conf. Electron. Inf. Emerg. Commun.*, 2019, pp. 1–7, doi: 10.1109/iceiec.2019.8784651.

[18] T. Bouguera, J. F. Diouris, J. J. Chaillout, R. Jaouadi, and G. Andrieux, "Energy consumption model for sensor nodes based on LoRa and LoRaWAN," *Sensors*, vol. 18, no. 7, 2018, doi: 10.3390/s18072104.

[19] Y. Zeng, J. Xu, and R. Zhang, "Rotary-wing UAV enabled wireless network: trajectory design and resource allocation," in *Proc. 2018 IEEE Glob. Commun. Conf. GLOBECOM*, doi: 10.1109/GLOCOM.2018.8647595.

[20] N. Aziemah, A. Ali, N. Adilah, A. Latiff, and I. S. Ismail, "Performance of LoRa network for environmental monitoring system in Bidong Island Terengganu, Malaysia," *Int. J. Adv. Comput. Sci. Appl.*, vol. 10, no. 11, pp. 127–134, 2019.

[21] M. Cattani, C. A. Boano, and K. Römer, "An experimental evaluation of the reliability of LoRa Long-Range low-power wireless communication," *Sens. Actuator Networks Artic.*, vol. 6, no. 7, 2017, doi: 10.3390/jsan6020007.

[22] B. Eric. (2019). *LoRa Documentation*. [Online]. Available: https://buildmedia.readthedocs.org/media/pdf/lora/latest/lora.pdf
[23] Y. Zeng, J. Xu, and R. Zhang, "Energy minimization for wireless communication with rotary-wing UAV," *IEEE Trans. Wirel. Commun.*, vol. 18, no. 4, pp. 2329–2345, 2019, doi: 10.1109/TWC.2019.2902559.
[24] Z. Yang, W. Xu, and M. Shikh-bahaei, *Energy Efficient UAV Communication With Energy Harvesting*, vol. 69, no. 2, pp. 1913–1927, 2020.
[25] C. Zhan and H. Lai, "Energy minimization in internet-of-things system based on rotary-wing UAV," *IEEE Wirel. Commun. Lett.*, vol. PP, no. c, pp. 1–1, 2019, doi: 10.1109/lwc.2019.2916549.
[26] Civil Aviation Authority Malaysia. (2019). CAAM Standard Requirement For The Application of Drone Permit (Below 20kg) [Online]. Available: www.mcmc.gov.my
[27] M. Juneja and S. K. Nagar, "Particle swarm optimization algorithm and its parameters: A review," in *Proc. 2016 Int. Conf. Control. Comput. Commun. Mater.*, pp. 1–5, 2016, doi: 10.1109/ICCCCM.2016.7918233.
[28] X. Zhang, D. Zou, and X. Shen, "A novel simple particle swarm optimization algorithm for global optimization," *Mathematics*, vol. 6, no. 287, 2018, doi: 10.3390/math6120287.
[29] B. Saji. (2021). In-depth intuition of k-means clustering algorithm in machine learning. [Online]. Available: https://www.analyticsvidhya.com/blog/2021/01/in-depth-intuition-of-k-means-clustering-algorithm-in-machine-learning/
[30] T. W. Bandeira and A. V Brito, *Analysis of Path Planning Algorithms Based on Travelling Salesman Problem Embedded in UAVs*, 2015, doi: 10.1109/SBESC.2015.20.